IEEE Access
Multidisciplinary | Rapid Review | Open Access Journal

Received March 11, 2019, accepted March 29, 2019, date of publication April 3, 2019, date of current version April 16, 2019.

Digital Object Identifier 10.1109/ACCESS.2019.2909049

Observer-Based Active Roll Preview Control With V2V Communication

JAEWON NAH[1] AND SEONGJIN YIM[2], (Member, IEEE)
[1]Department of Automotive Engineering, Honam University, Gwangju 62399, South Korea
[2]Department of Mechanical and Automotive Engineering, Seoul National University of Science and Technology, Seoul 01811, South Korea

Corresponding author: Seongjin Yim (acebtif@seoultech.ac.kr)

This work was supported by the Research Program funded by the Seoul National University of Science and Technology.

ABSTRACT This paper presents observer-based active roll preview control with V2V communication. The preview controllers are designed with a future disturbance, transmitted lateral acceleration from preceding vehicles with V2V communication. For active roll control, two preview controllers—LQ and H_∞ ones—are designed with the linear roll model. Generally, it is hard to measure the roll angle in real vehicles. To estimate the roll angle, Kalman filter is adopted with the roll rate measurement. To filter the noises in the transmitted lateral acceleration, a moving average filter is adopted. To validate the proposed method, simulation is done on a vehicle simulation package. From the simulation, it is shown that the proposed method is effective in estimating the roll angle and in filtering the noises in the transmitted lateral acceleration.

INDEX TERMS Active roll control, Kalman filter, preview control, V2V communication.

I. INTRODUCTION

The aim of active roll control(ARC) is to reduce the roll angle and the roll rate caused by road profile or lateral acceleration for ride comfort and rollover prevention [1]. The disturbance in ARC is the lateral acceleration caused by excessive steering or severe cornering. So, the purpose of ARC is to attenuate an effect of lateral acceleration on the roll angle and the roll rate of vehicles. There have been two types of active actuators used for ARC: active suspension and active anti-roll bar (Active ARB) [2]. Semi-active actuators such as continuous damping control was not considered in this paper. In this paper, only the active ARB is used as an actuator for ARC.

There have been several researches on the control of ARC [3]–[7]. Most of these researches have used only feedback control with the roll angle and the roll rate. Generally, it is not easy to measure the roll angle of vehicles in real road environment. Moreover, a roll angle sensor is quite expensive. So, a state observer has been used to estimate the roll angle with the roll rate measurement [4]–[9]. In the previous research, LQG-LTR was adopted for estimating the roll angle with the roll rate measurement [4]. The open-loop observer was proposed to calculate the roll angle and roll rate with the lateral acceleration measurement [7]. Recently, neural networks and nonlinear observer have been adopted for roll angle estimation [8], [9]. Generally, the roll rate can be measured by a sensor. Several types of the roll rate sensors have been published up to date [10], [11]. With the measurement of the roll rate, the roll angle can be estimated using Kalman filter. Following the idea in the previous researches, the discrete-time Kalman filter is adopted for roll angle estimation in this paper.

Compared to the feedback control as PD-control and linear quadratic regulator (LQR) used in ARC, the feedforward control with the measured lateral acceleration has been adopted in a small number of researches [12], [13]. Once the feedforward control is used with the lateral acceleration, it outperformed the feedback control. Thus, it is desirable to use the feedforward control as much as possible for ARC. Typical approach that uses the feedforward control from measured disturbances is preview control. Preview control uses the feedforward control input with measured future disturbances to enhance performance of control system. Typical case of preview control is active suspension control for ride comfort and cornering [14]. However, in previous works, the preview control has not been applied to ARC because the future lateral acceleration cannot be measured or estimated. Recent researches in intelligent transportation technologies (ITS) make vehicles communicate with other through V2V communication. With V2V communication, a vehicle can get the future lateral acceleration from preceding ones. With the future distances, preview control can be applied as shown in [12]–[15]. Rahman and Rideout applied the LQ optimal preview control to active suspension control for ride comfort with the future road profile transmitted from the leading

The associate editor coordinating the review of this manuscript and approving it for publication was Zhengbing He.

vehicle in vehicle convoy [14]. Yim applied LQ optimal preview control to yaw and roll motion control for vehicle stability and active roll stabilization [12], [13]. In those previous works, V2V communication was adopted to obtain the future disturbances such as the road profile or the lateral acceleration in the following vehicles.

Active roll preview control uses the lateral acceleration data, which are transmitted from the preceding vehicles through V2V communication [12], [13]. Under actual vehicle driving conditions, there are a large amount of noises on the transmitted lateral acceleration. There are two types of noise sources in the lateral acceleration data. The first type of noise source is the on-board sensors in actual vehicles. It is well-known that signals obtained from commercial sensors installed on passenger cars has a large amount of noises [16]. So, in general, the filtered lateral acceleration signal has been used for control purpose. The second type of noise source is the packet loss and the signal distortion in communication. According to the previous work [17], the packet loss rate drastically increases as the transmission rate and the packet size do. In preview control, the noises in the future disturbances have a large effect on the control performance. In other words, the feedforward control input is directly affected by the noises in the future disturbances. So, it is necessary to filter the noises. For the purpose, a moving average filter is adopted in this paper.

In summary, the contributions of this paper are to apply a discrete-time Kalman filter to estimate the roll angle with roll rate measurement and to filter a noisy lateral acceleration transmitted between vehicles with a moving average filter.

This paper is divided into the following parts. In section 2, two preview controllers – LQ and H_∞ preview controllers – are designed with linear model. In section 3, the method of constructing a future disturbance with V2V communication is presented. The discrete-time Kalman filter (DTKF) is designed to estimate the roll angle, and a moving average filter is applied to filter noises in the transmitted lateral acceleration. In section 4, simulation is done with the designed observer-based preview controllers on a vehicle simulation package, CarSim. The conclusion is presented in Section 5.

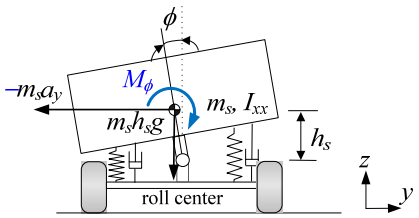

FIGURE 1. DOF roll model.

II. DESIGN OF ACTIVE ROLL PREVIEW CONTROLLERS

A. DERIVATION OF AUGMENTED STATE-SPACE EQUATION

To design a controller for roll motion in this paper, 1-DOF linear model, as shown in Fig. 1, is used [7], [12], [13]. This simple model describes the roll motion of a vehicle. The control input is the control roll moment M_ϕ acting on the front and rear axles, generated by an active ARB. The disturbance is the lateral acceleration a_y that causes the roll motion of a vehicle. The equation of the motion is derived as (1). With the definition of state vector (2), the continuous-time state-space equation is derived as (3). The discrete-time state-space equation (4) can be obtained by discretizing (3) with the sampling time T_s [12], [13].

$$I_{xx}\ddot{\phi}(t) + B_\phi\dot{\phi}(t) + K_\phi\phi(t) - m_s h_s a_y(t) - m_s g h_s \phi(t) = M_\phi(t) \tag{1}$$

$$\mathbf{x}(t) \equiv \begin{bmatrix} \phi(t) & \dot{\phi}(t) \end{bmatrix}^T \tag{2}$$

$$\begin{aligned} \dot{\mathbf{x}}(t) &= \mathbf{A}\mathbf{x}(t) + \mathbf{B}_1 a_y(t) + \mathbf{B}_2 M_\phi(t) \\ &= \begin{bmatrix} 0 & 1 \\ -\dfrac{K_\phi - m_s g h_s}{I_{xx}} & -\dfrac{B_\phi}{I_{xx}} \end{bmatrix} \mathbf{x}(t) + \begin{bmatrix} 0 \\ \dfrac{1}{I_{xx}} \end{bmatrix} a_y(t) \\ &\quad + \begin{bmatrix} 0 \\ \dfrac{m_s h_s}{I_{xx}} \end{bmatrix} M_\phi(t) \end{aligned} \tag{3}$$

$$\mathbf{x}(k+1) = \mathbf{\Phi}\mathbf{x}(k) + \mathbf{\Gamma} a_y(k) + \mathbf{\Omega} M_\phi(k) \tag{4}$$

Let the preview interval T_p, which is defined as $p \cdot T_s$. Let $\mathbf{\Theta}(k)$ be the vector of the measured a_y at future instant k, as presented in (5). The state-space equation of $\mathbf{\Theta}(k)$ can be derived as (6). In (6), the definitions of the matrices $\mathbf{\Pi}$ and $\mathbf{\Xi}$ can be found in [12]. When designing a preview controller, it is convenient to use the augmented state vector $\sigma(k) = [\mathbf{x}(k) \quad \mathbf{\Theta}(k)]^T$. With the definition of $\sigma(k)$, the augmented state-space equation is derived as (7) [15]. In (7), $\mathbf{\Lambda} \equiv [\mathbf{\Gamma}\ \mathbf{0}\ \ldots\ \mathbf{0}]$.

$$\mathbf{\Theta}(k) = \begin{bmatrix} a_y(k) & a_y(k+1) & \cdots & a_y(k+p) \end{bmatrix}^T \tag{5}$$

$$\mathbf{\Theta}(k+1) = \mathbf{\Pi}\mathbf{\Theta}(k) + \mathbf{\Xi} a_y(k+p+1) \tag{6}$$

$$\begin{aligned} \boldsymbol{\sigma}(k+1) &= \begin{bmatrix} \mathbf{\Phi} & \mathbf{\Lambda} \\ \mathbf{0} & \mathbf{\Pi} \end{bmatrix} \boldsymbol{\sigma}(k) + \begin{bmatrix} \mathbf{0} \\ \mathbf{\Xi} \end{bmatrix} a_y(k+p+1) \\ &\quad + \begin{bmatrix} \mathbf{\Omega} \\ \mathbf{0} \end{bmatrix} M_\phi(k) \end{aligned} \tag{7}$$

B. DESIGN OF LQ OPTIMAL PREVIEW CONTROLLER

LQ optimal control is the most common method in designing a preview controller [12]–[15]. LQ cost function J for the roll motion control is given as (8). The weights ρ_i of J are set by $\rho_i = 1/\eta_i^2$, where η_i represents the maximum allowable value of each weight in J [13].

$$J = \sum_{k=0}^{\infty} \left[\rho_1 \phi^2(k) + \rho_2 \dot{\phi}^2(k) + \rho_3 M_\phi^2(k) \right] \tag{8}$$

The LQ cost function (8) can be converted into the following form:

$$J = \sum_{k=0}^{\infty} \mathbf{z}^T(k)\mathbf{z}(k) = \sum_{k=0}^{\infty} \left[\mathbf{x}^T(k)\mathbf{L}\mathbf{x}(k) + r M_\phi^2(k) \right]$$

$$\mathbf{z}(k) = \mathbf{M}\mathbf{x}(k) + \mathbf{N}u(k), \quad \mathbf{L} \equiv \mathbf{M}^T\mathbf{M}, \quad r \equiv \mathbf{N}^T\mathbf{N}, \quad (9)$$

where

$$\mathbf{M} = \begin{bmatrix} \sqrt{\rho_1} & 0 \\ 0 & \sqrt{\rho_2} \\ 0 & 0 \end{bmatrix}, \quad \mathbf{N} = \begin{bmatrix} 0 \\ 0 \\ \sqrt{\rho_3} \end{bmatrix}$$

LQR is obtained as the form of the full-state feedback control: $M_\phi(k) = -\mathbf{K}_{LQR}\mathbf{x}(k)$. To use full-state feedback controller, it is necessary to measure the state variables. It is not difficult to measure the roll rate. However, the roll angle is hard to measure. So, it should be estimated with some observers. For the purpose, a discrete-time Kalman filter (DTKF) is used for the purpose of estimation in this paper.

Following the definition of the augmented state vector $\sigma(k)$, the LQ cost function (9) should be converted to (10). The LQR with the augmented system (7) and the converted LQ cost function (10) is obtained as (11).

$$\bar{J} = \sum_{k=0}^{\infty} \left\{ \boldsymbol{\sigma}^T(k) \begin{bmatrix} \mathbf{L} & \mathbf{0} \\ \mathbf{0} & 0 \end{bmatrix} \boldsymbol{\sigma}(k) + rM_\phi^2(k) \right\} \quad (10)$$

$$\begin{aligned} M_\phi(k) &= -\mathbf{K}_{LQ}\boldsymbol{\sigma}(k) \\ &= -\begin{bmatrix} \mathbf{K}_{LQ,FB} & \mathbf{K}_{LQ,FF} \end{bmatrix} \begin{bmatrix} \mathbf{x}(k) \\ \Theta(k) \end{bmatrix} \end{aligned} \quad (11)$$

The gain $\mathbf{K}_{LQ}$ of LQ optimal preview controller can be obtained from Riccatti equation. In (11), $\mathbf{K}_{LQ,FB}$ and $\mathbf{K}_{LQ,FF}$ represent the feedback and feedforward gains, respectively. The notable feature is that the feedback gain of LQ preview controller, $\mathbf{K}_{LQ,FB}$, is identical to that of LQR, $\mathbf{K}_{LQR}$.

C. DESIGN OF H_∞ OPTIMAL PREVIEW CONTROLLER

H_∞ control has been known as a disturbance attenuation controller. So, it is relevant to ARC under the lateral acceleration. The discrete-time H_∞ preview controller is designed in this paper.

With the feedback control $M_\phi(k) = \mathbf{K}_\infty\mathbf{x}$, the L_2 gain for the system (4) is said to be attenuated by γ if the following condition is satisfied.

$$\frac{\sum_{k=0}^{\infty} \mathbf{z}^T(k)\mathbf{z}(k)}{\sum_{k=1}^{\infty} a_y^2(k)} = \frac{\sum_{k=0}^{\infty} \left[\mathbf{x}^T(k)\mathbf{L}\mathbf{x}(k) + rM_\phi^2(k) \right]}{\sum_{k=1}^{\infty} a_y^2(k)} \leq \gamma^2 \quad (12)$$

To find the feedback controller gain $\mathbf{K}_\infty$ which can give the minimum γ, the linear matrix inequality (LMI) (13) is adopted [18], [19]. From the solutions $\mathbf{Y}$ and $\mathbf{Z}$ obtained by solving LMI optimization problem (13), the feedback controller gain $\mathbf{K}_\infty$ is derived as $\mathbf{K}_\infty = \mathbf{Z}\mathbf{Y}^{-1}$. If the identical form of LMI is applied to the augmented system (7), the H_∞ preview controller can be derived, which has the same structure as (11). The notable feature is that the feedforward gain of LQ and H_∞ optimal controllers are identical, $\mathbf{K}_{LQ,FF}$ as given in (11). This is natural because the LQ objective function, (9), is used as the performance measure (12) of H_∞ control.

$$\begin{aligned} &\min_{\mathbf{Y},\mathbf{H},\gamma} \ \gamma \\ &\mathbf{Y} > 0, \quad \gamma > 0 \\ &s.t. \begin{bmatrix} -\mathbf{Y} & \boldsymbol{\Phi}\mathbf{Y} + \boldsymbol{\Omega}\mathbf{H} & \Gamma & \mathbf{0} \\ * & -\mathbf{Y} & \mathbf{0} & (\mathbf{M}\mathbf{Y} + \mathbf{N}\mathbf{H})^T \\ * & * & -\gamma\mathbf{I} & \mathbf{0} \\ * & * & * & -\gamma\mathbf{I} \end{bmatrix} < 0 \end{aligned} \quad (13)$$

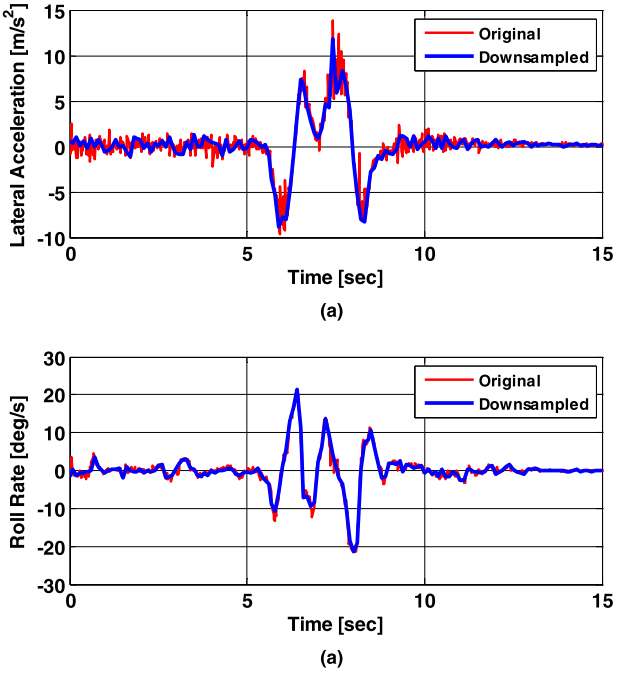

FIGURE 2. Measured lateral acceleration and roll rate on a real vehicle. (a) Lateral acceleration. (b) Roll rate.

III. OBSERVER DESIGN AND NOISE FILTERING

A. NECESSITY OF NOISE FILTERING

Recently, commercial sensors have been published for roll rate measurement. Fig. 2 shows the lateral acceleration and roll rate measured from HG1120 of HoneyWell Aerospace on a double lane change maneuver. The sampling time of HG1120 is 20ms. In Fig. 2, the red line shows the signals measured with the sampling time of 20ms. The blue line shows the signals down-sampled with the sampling time of 100ms. As shown in Fig. 2, the original lateral acceleration signal is quite noisy. On the other hand, the down-sampled signal of that is less noisy. However, the down-sampling has been not recommended because it make an original signal lose useful information. So, the original signal, not the down-sampled one, should be filtered for control purpose.

B. METHOD TO OBTAIN FUTURE LATERAL ACCELERATION WITH V2V COMMUNICATION

Using V2V communication, sensor signals on a vehicle can be transmitted to others. The transmitted information can be

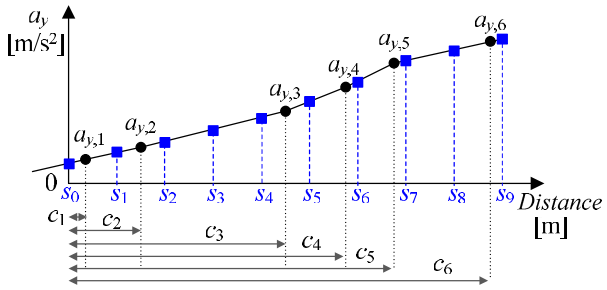

FIGURE 3. Interpolation with distance-based lateral acceleration data.

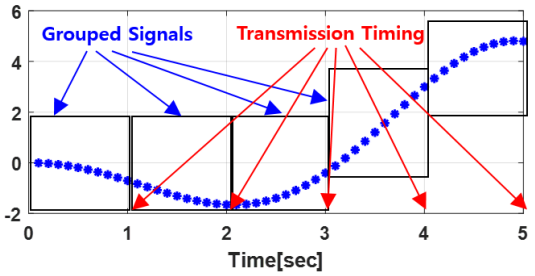

FIGURE 4. Measured lateral acceleration and roll rate on a real vehicle.

used to predict and prepare for situation in a few seconds. In case of roll motion control, the upcoming lateral acceleration data from a preceding vehicle can be utilized for preview control.

From the preceding vehicle, position information and lateral acceleration measured by high-precision DGPS and an accelerometer, respectively, are transmitted to the following vehicles. The measured position data, i.e., the points, are on the trajectory of the preceding vehicle. Using the preceding vehicle position, the inter-point distances d can be acquired on the following vehicle. Thus the cumulative distances, c_i in Fig. 3, from the current position of the following vehicle to i-th position on the trajectory of the preceding one can be known, as given in (14). For each c_i, the transmitted lateral acceleration $a_{y,i}$ from the preceding vehicle is marked in Fig. 3. In this paper, the marked $a_{y,i}$ is defined as distance-based lateral acceleration.

In (15), s_p stands for a query point for interpolation, while $v(k)$ stands for speed of the following vehicle at k-th step. As shown in (15), the gap between query points equals to $v(k)$-T_s assuming that $v(k)$ is constant during the preview time T_p. Linear interpolation, i.e., distance-based interpolation [12], [13] which has been adopted to resample the time-based lateral acceleration from the distance-based should be done for each sampling time T_s. With the distance-based interpolation, the preview controller can treat the change of vehicle speed. Further, the distance-based interpolation can treat circumstances with packet losses of V2V communication. The influence of the packet loss in V2V has been investigated in the previous research [15].

$$c_i = \sum_{j=1}^{i} d_j \tag{14}$$

$$\begin{aligned} \mathbf{S} &= \begin{bmatrix} S_0 & S_1 & S_2 & S_3 & \cdots & S_{p-1} & S_p \end{bmatrix} \\ &= v(k) \times \begin{bmatrix} 0 & T_s & 2T_s & 3T_s & \cdots & (p-1)T_s & pT_s \end{bmatrix} \end{aligned} \tag{15}$$

Generally, the transmission rate of V2V communication is set to the maximum among the sampling rates of sensors and the transmission rate of the communication device. For example, the sampling rates of a gyroscope, an accelerometer and a GPS are assumed to be 20ms, 10ms and 100ms, respectively. The transmission rate of a commercial device is 20ms [20]. Then, the transmission rate is to be set to 100ms, which is the maximum of these devices. As a result, the signal from a gyroscope and an accelerometer should be down-sampled with the sampling rate of 100ms. This means the information loss.

To transmit the original signal without information loss, signals with the high sampling rate is grouped according to low sampling rate, and the group is transmitted via V2V communication. For example, 10 consecutive signals of the lateral acceleration are grouped according to the sampling rate 100ms of GPS. After receiving the group signal, it can be easily constructed to the original one. Fig. 4 illustrates this method.

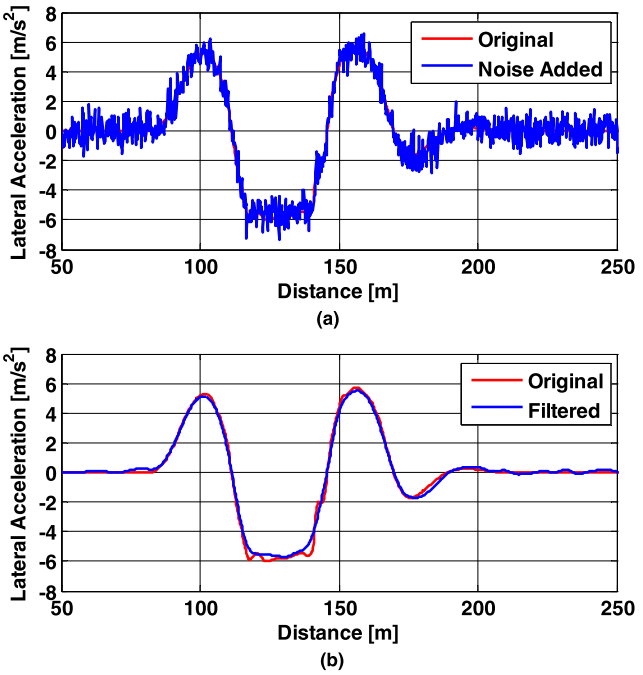

FIGURE 5. Transmitted lateral acceleration from the preceding vehicle. (a) Lateral acceleration transmitted from preceding vehicle. (b) Filtered lateral acceleration with moving average filter.

C. NOISE FILTERING ON THE TRANSMITTED LATERAL ACCELERATION

Generally, there are a lot of filters used for noise filtering. In this paper, a simple moving average filter is used for noise filtering. Generally, a noise filtering is applied in real-time manner. As a result, it causes a time delay in filtered signals. When using V2V communication, there is a period

of traveling time until the actual disturbance measured in the preceding vehicle is applied to the following one. So, a noise filtering on the transmitted signal can be done during the period. Consequently, there are no delays in filtering the signal. Fig. 5 shows the original and the filtered lateral acceleration signals. The original signal was transmitted from the preceding vehicle which did a double lane change maneuver [12], [13]. In Fig. 5, the original signal is represented by the red line. White noise with the variance of 1e-6 has been added into the original signal, which is represented by the blue line. Fig. 5-(b) shows the filtering results of the moving average filter with the filter length of 30. As shown in Fig. 5-(b), there are no delays in the filtered lateral acceleration, and it is good enough to be used for preview control.

D. DESIGN OF ROLL ANGLE ESTIMATOR

In this subsection, a state estimator or Kalman filter is designed to estimate the roll angle with the roll rate measurement. The state-space equation (4) is used for Kalman filter design. In the equation of motion (1), the most important parameters are the roll stiffness K_ϕ and the roll damping B_ϕ. These parameters have been identified from experimental data by the optimization procedure, given in [7]. Because the measurement for the Kalman filter is the roll rate, the output equation is given in (16). In (16), $\mathbf{w}(k)$ and $\mathbf{v}(k)$ are a zero-mean white-noise processes of system uncertainty and measurement noise, respectively. The corresponding covariance matrices are given in (17).

$$\begin{cases} \mathbf{x}(k+1) = \mathbf{\Phi}\mathbf{x}(k) + \mathbf{\Gamma} a_y(k) + \mathbf{\Omega} M_\phi(k) + \mathbf{w}(k) \\ \mathbf{y}(k) = \mathbf{C}\mathbf{x}(k) + \mathbf{v}(k) = \begin{bmatrix} 0 & 1 \end{bmatrix} \mathbf{x}(k) + \mathbf{v}(k) \end{cases} \tag{16}$$

$$\mathbf{W}(k) = E\left\{\mathbf{w}(k)\mathbf{w}^T(k)\right\}, \quad \mathbf{V}(k) = E\left\{\mathbf{v}(k)\mathbf{v}^T(k)\right\} \tag{17}$$

The discrete-time Kalman filter (DTKF) has the form of the time and measurement updates, as given in (18) and (19), respectively. The covariance matrices of system uncertainty and measurement noise are used to tune the performance of the Kalman filter. For example, if $\mathbf{W}$ is set to large values, then the Kalman filter emphasizes more the sensor measurement than the system dynamics. On the other hand, if $\mathbf{V}$ is set to large, the Kalman filter emphasizes more the system dynamics than the sensor measurement. With the state estimator, the state vector $\mathbf{x}(k)$ is replaced with the estimated one, $\hat{\mathbf{x}}(k)$, in the preview controllers.

$$\begin{cases} \hat{\mathbf{x}}_-(k) = \mathbf{\Phi}\hat{\mathbf{x}}(k-1) + \mathbf{\Gamma} w(k-1) + \mathbf{\Omega} u(k-1) \\ \mathbf{P}_-(k) = \mathbf{W}(k) + \mathbf{\Phi}\mathbf{P}(k-1)\mathbf{\Phi}^T \end{cases} \tag{18}$$

$$\begin{cases} \mathbf{K}_e = \mathbf{P}_-(k)\mathbf{C}^T\left[\mathbf{V}(k) + \mathbf{C}\mathbf{P}_-(k)\mathbf{C}^T\right] \\ \hat{\mathbf{x}}(k) = \hat{\mathbf{x}}_-(k) + \mathbf{K}_e\left[\mathbf{y}(k) - \mathbf{C}\hat{\mathbf{x}}_-(k)\right] \\ \mathbf{P}(k) = (\mathbf{I} - \mathbf{K}_e\mathbf{C})\,\mathbf{P}_-(k) \end{cases} \tag{19}$$

The signal from the roll rate sensor is noisy. In the case, the control input is directly influenced by the noise because of the full-state feedback control. So, it should be filtered. In this paper, Kalman filter with constant velocity model (KFCVM) is adopted for noise filtering. The discrete-time state-space equation of constant velocity model is given in (20). In (20), $x(k)$ is the displacement. In (20), $\chi(k)$ and $\zeta(k)$ are the vectors of white-noise processes representing the system uncertainty and measurement noise, respectively. The covariance matrices of the system uncertainty and measurement noise are given in (21). The tuning parameters of the Kalman filter are the variances σ_p^2 and σ_r^2 of the system uncertainty and measurement noise, respectively.

$$\begin{bmatrix} \dot{x}(k+1) \\ \ddot{x}(k+1) \end{bmatrix} = \begin{bmatrix} 1 & T_s \\ 0 & 1 \end{bmatrix} \begin{bmatrix} x(k) \\ \dot{x}(k) \end{bmatrix} + \chi(k)$$
$$y(k) = \begin{bmatrix} 1 & 0 \end{bmatrix} \begin{bmatrix} x(k) \\ \dot{x}(k) \end{bmatrix} + \zeta(k) \tag{20}$$

$$\mathbf{X} = \sigma_q^2 \begin{bmatrix} T_s^3/3 & T_s^2/2 \\ T_{s/2}^2 & T_s \end{bmatrix}, \quad \mathbf{Z} = \sigma_r^2 \tag{21}$$

IV. SIMULATION

In this section, simulation was done on CarSim to evaluate three preview controllers, the roll angle estimator and 1st-order exponential smoothing filter.

TABLE 1. Parameters of the 1-DOF roll model.

m_s	984.0 kg	h_s	0.625 m
I_{xx}	442.0 kg·m^2	B_ϕ	6,486 N·s/m
K_ϕ	76,073 N/m		

TABLE 2. Maximum allowable values in LQ cost function.

η_1	1 deg	η_2	10 deg/s	η_3	1500 Nm

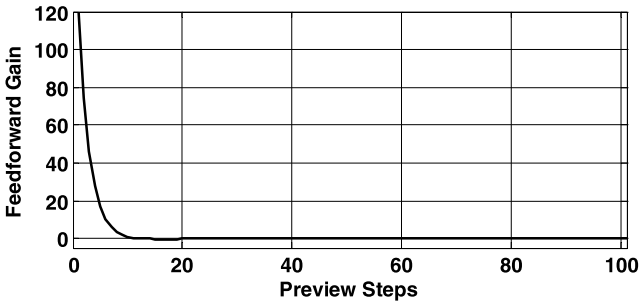

FIGURE 6. Feedforward gains for each preview step.

The parameters of the linear roll model were obtained from CarSim, as presented in Table 1. The weights in J and the variances of system uncertainty and measurement noise are given in Table 2 and Table 3, respectively. The sampling time and the preview interval of the preview controllers were set to be 10ms and 1sec, respectively. This means the preview length is 101. Three preview controllers and the roll angle estimator were implemented on MATLAB/ Simulink. The gain matrices of LQ and H_∞ preview controllers are given in (22). The values of feedforward gain are given in Fig. 6. As mentioned earlier, two preview controllers use identical feedforward gains. As shown in Fig. 6, the feedforward control has little effect on the preview control over 10 preview

TABLE 3. Variances of system uncertainty and measurement noise.

$\mathbf{W}(k)$	$\begin{bmatrix} 1e-4 & 0 \\ 0 & 1e+4 \end{bmatrix}$	$\mathbf{V}(k)$	1e–4

steps with the sampling time of 10ms. In other words, it is enough to use the feedforward control with the preview period of 100ms under the sampling time of 10ms.

$$\mathbf{K}_{LQ,FB} = \begin{bmatrix} 61407 & 6514 \end{bmatrix}$$
$$\mathbf{K}_{\infty} = \begin{bmatrix} 117660 & 16903 \end{bmatrix} \quad (22)$$

The simulation scenario was the closed-loop steering with a driver model on the moose test track [12], [13]. The driver model, given in CarSim, was used in the simulation. The initial vehicle speed was set to 80km/h or 22.2m/s, and the tire-road friction coefficient was set to 0.6. The vehicle loses its lateral stability if no yaw motion controllers are applied. So, this is a severe double lane change maneuver. As pointed in the previous work, the yaw and roll motion controllers can be designed separately [21]. So, the integrated chassis control (ICC) with electronic stability control (ESC) and active front steering (AFS) was implemented [22]. The active ARB was adopted as an actuator for roll moment generation. The actuator model for active ARB was the first-order system with the time constant of 0.05. The simulation interval was set to 10secs.

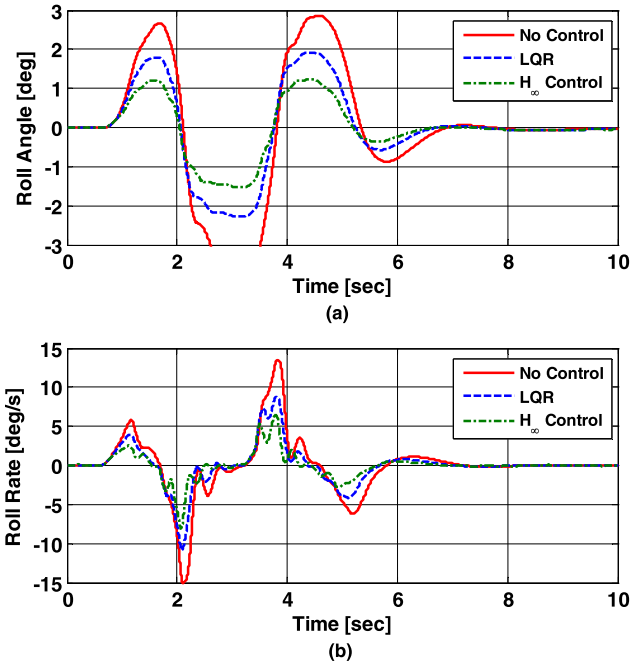

FIGURE 7. Simulation results of feedback controllers with roll angle estimator. (a) Roll angle. (b) Roll rate.

A. PERFORMANCE EVALUATION OF ROLL ANGLE ESTIMATOR

In this subsection, the performance of the roll angle estimator is evaluated on CarSim. LQR and H_∞ feedback controllers

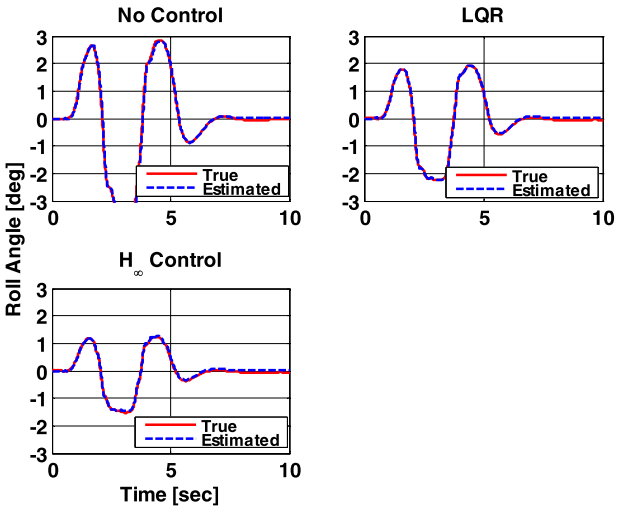

FIGURE 8. Estimation results of the roll angle estimator with feedback controllers.

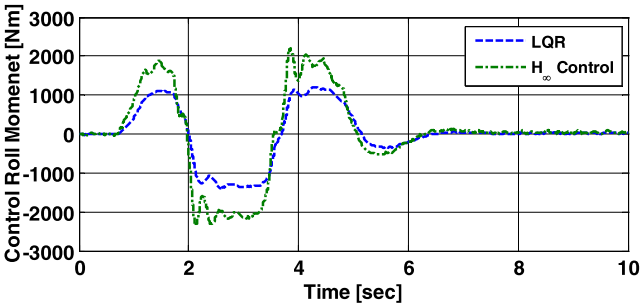

FIGURE 9. Control inputs for three preview controllers.

are applied for active roll control. For realistic simulation, a white noise with the variance of 1e-7 is added to the roll rate signal. For noise filtering, KFCVM is applied to the roll rate signal. Figs. 7, 8, and 9 show the simulation results, the estimation results of control inputs of feedback controllers, respectively. As shown in Figs. 7 and 8, H_∞ controller gives the best result for ARC. However, there is chattering in control roll moments, as shown in Fig. 9. In spite of that, there is no chattering in the response of the roll angle and the roll rate for H_∞ controller. This is caused by the fact that the roll motion has slow dynamics. As shown in Fig. 9, the roll angle estimator gives good estimation results under the measurement noise in the roll rate signal. From these results, it can be concluded that the discrete-time Kalman filter gives good performance in estimating the roll angle.

B. PERFORMANCE EVALUATION OF PREVIEW CONTROLLERS

In this subsection, the performance of three preview controllers is evaluated. The lateral acceleration measured on a preceding vehicle is transmitted to a following one [12], [13]. Fig. 10 shows the lateral acceleration and the vehicle speed measured on the preceding vehicle. The initial inter-vehicle gap was set to 22.2m. To resample the previewed disturbances according to the speed change, the distance-based

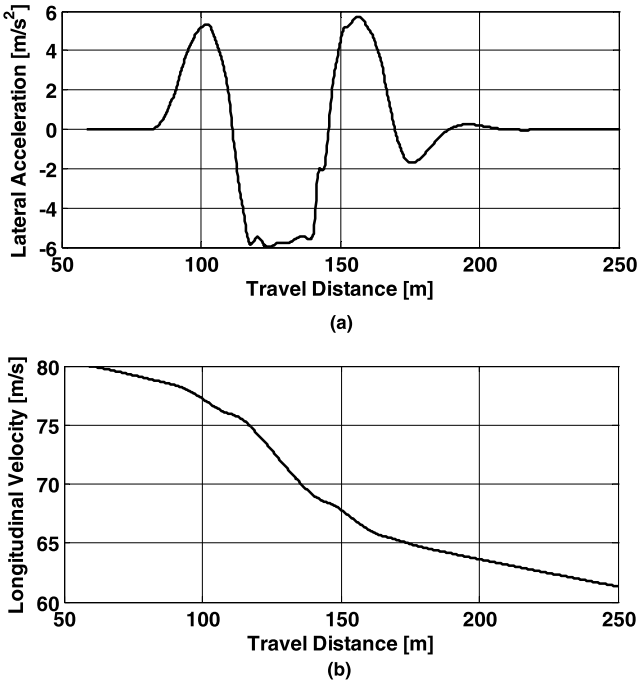

FIGURE 10. Simulation results with CarSim driver model on the moose test track. (a) Lateral acceleration of the preceding vehicle. (b) Vehicle Speed of the preceding vehicle.

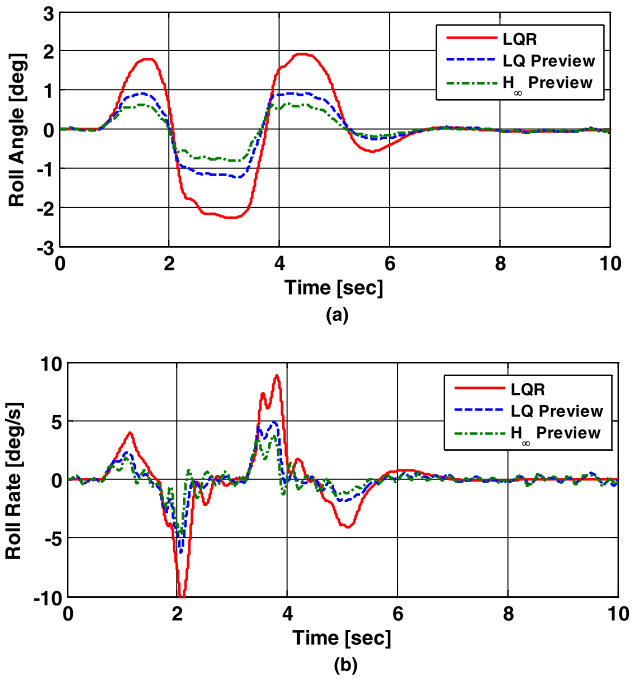

FIGURE 11. Simulation results of preview controllers without filtering. (a) Roll angle. (b) Roll rate.

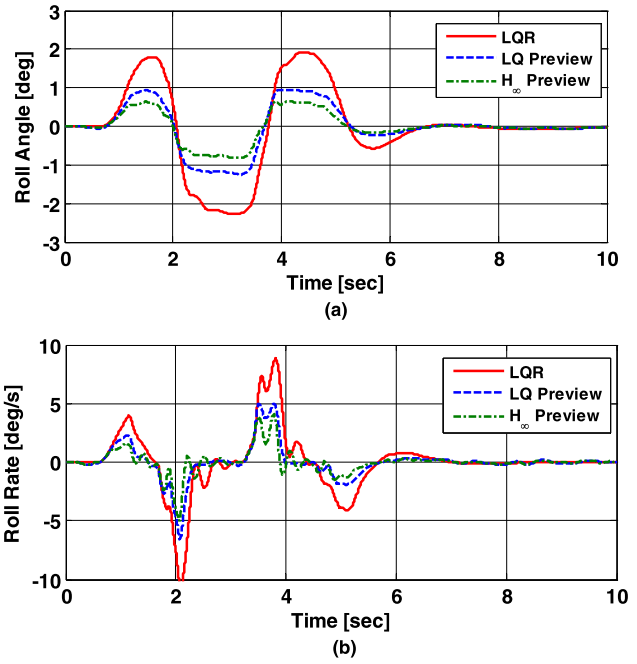

FIGURE 12. Simulation results of preview controllers with filtering. (a) Roll angle. (b) Roll rate.

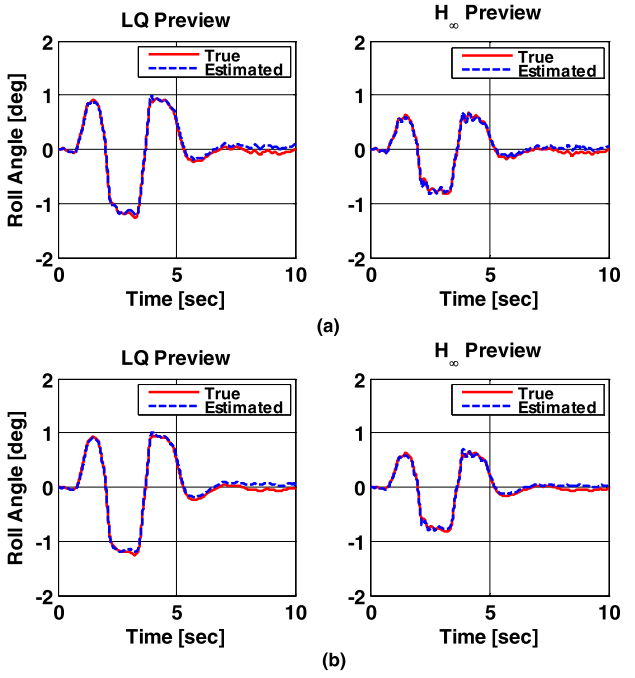

FIGURE 13. Roll angle estimation results for the cases with and without filtering. (a) Roll angles without filtering. (b) Roll angles with filtering.

interpolation on the following vehicle was applied. The transmission interval of V2V communication device was set to 100ms.

Figs. 11 and 12 show the roll angles and roll rates for each preview controller with and without filtering on the transmitted lateral acceleration, respectively. Fig. 13 shows the performance of the roll angle estimator for cases with filtering and without filtering. Fig. 14 shows the control roll moments of feedback and feedforward parts. In Fig. 14, the legends FB and FF represent the feedback and feedforward control inputs, respectively. As shown in Fig. 14, the feedforward inputs of three preview controllers are identical because of the same feedforward gain.

As shown in Figs. 11 and 12, the relative performances of two preview controllers are similar to those in the cases with

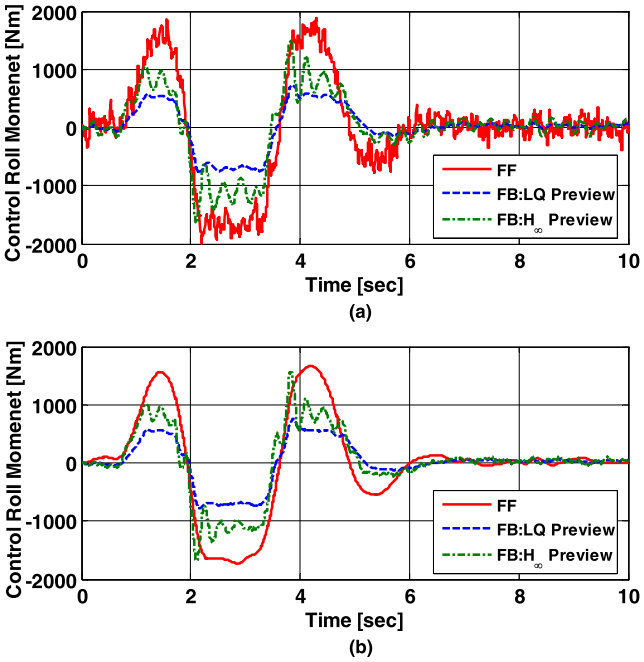

FIGURE 14. Feedback and feedforward inputs of preview controllers. (a) Without filtering on transmitted lateral acceleration. (b) With filtering on transmitted lateral acceleration.

TABLE 4. The maximum absolute values of roll angle and roll rate for the case without filtering.

	Maximum Roll Angle (deg)	Maximum Roll Rate (deg/sec)	Maximum M_ϕ (N·m)
LQR	2.26	10.93	1390
LQ Preview	1.27	6.33	2725
H_∞ Preview	0.83	4.82	3235

TABLE 5. The maximum absolute values of roll angle and roll rate for the case with filtering.

	Maximum Roll Angle (deg)	Maximum Roll Rate (deg/sec)	Maximum M_ϕ (N·m)
LQR	2.26	10.93	1390
LQ Preview	1.25	6.58	2414
H_∞ Preview	0.82	5.10	3028

filtering and without filtering. As mentioned in the previous subsection, this can be explained by the fact that the roll motion has slow dynamics. So, it plays a role of low-pass filter against the high-frequency inputs. Performance of the state estimator is good regardless of the cases with filtering and without filtering, as shown in Fig. 13. However, there are chattering for the case without filtering on the lateral acceleration. The chattering in the roll rate is more severe than that in the roll angle. This can be explained by the fact that the noise in the lateral acceleration has a direct effect on the feedforward input, as shown in Fig. 14. As shown in Fig. 14-(a), in the case without filtering, the feedback inputs fluctuate according the noisy feedforward inputs. On the other hand, this is reduced by filtering the transmitted lateral acceleration, as shown in Fig. 14-(b).

Table 4 and 5 show the maximum absolute values of the roll angle, the roll rate and the control roll moment of the simulations as shown in Figs. 11, 12 and 14, respectively. As shown in these results, the roll angle and roll rate of the vehicle can be reduced by three preview controllers. Moreover, the maximum control roll moments are reduced by filtering on the transmitted lateral acceleration, compared to the case without filtering. Among these three preview controllers, the H_∞ preview controller shows the best performance. However, the control roll moment calculated by H_∞ the preview controller is larger than that of the other two controllers, as shown in Table 4 and 5.

V. CONCLUSION

In this paper, the discrete-time Kalman fitler with the roll rate measurement was adopted as a roll angle estimator for ARC. With the transmitted lateral acceleration from preceding vehicles, two preview controllers – LQ and H_∞ ones – for ARC were designed for better control performance. To filter the transmitted lateral acceleration form preceding vehicles, a moving average filter without delays was applied. To investigate the performance of the designed controllers, simulation via CarSim has been conducted. The results of the simulation show that the roll angle estimator was good enough to be applied to real vehicles, and that the filtering on the transmitted lateral acceleration has reduced the magnitude of the control roll moment. In this research, parameters e.g., mass and inertia were regarded as a fixed constant. Future work will include parameter estimation and validation via real vehicle driving. Additionally, performance of the proposed roll angle estimator will be investigated via real vehicle, compared to GPS/IMU data.

NOMENCLATURE

a_y	lateral acceleration (m/s^2)
B_ϕ	roll damping coefficient (N·m·s/rad)
g	gravitational acceleration (9.81 m/s^2)
h_s	height of C.G. from a roll center (m)
I_{xx}	roll moment of inertia about roll axis (kg·m^2)
K_ϕ	roll stiffness (N·m/rad)
M_ϕ	control roll moment (N·m)
m_s	sprung mass of a vehicle (kg)
p	preview length
T_s	sampling period (sec)
T_p	preview period (sec)
ρ	weights in LQ objective function
ϕ	roll angle (rad)
$\dot{\phi}$	roll rate (rad/s)

REFERENCES

[1] A. Sorniotti, A. Morgando, and M. Velardocchia, "Active roll control: System design and hardware-in-the-loop test bench," *Vehicle Syst. Dyn.*, vol. 44, pp. 489–505, Jan. 2006.

[2] Y. Mizuta, M. Suzumura, and S. Matsumoto, "Ride comfort enhancement and energy efficiency using electric active stabiliser system," *Vehicle Syst. Dyn.*, vol. 48, no. 11, pp. 1305–1323, 2010.

[3] H. J. Kim and Y. P. Park, "Investigation of robust roll motion control considering varying speed and actuator dynamics," *Mechatronics*, vol. 14, pp. 35–54, Feb. 2004.

[4] D. J. M. Sampson and D. Cebon, "Active roll control of single unit heavy road vehicles," *Vehicle Syst. Dyn.*, vol. 40, no. 4, pp. 229–270, 2003.
[5] Y. Ohta *et al.*, "Development of an electric active stabilizer system based on robust design," SAE, Warrendale, PA, USA, Tech. Rep. 2006-01-0758, 2006.
[6] K. Jeon, H. Hwang, S. Choi, J. Kim, K. Jang, and K. Yi, "Development of an electric active rollcontrol (ARC) algorithm for a SUV," *Int. J. Automot. Technol.*, vol. 13, no. 2, pp. 247–253, 2012.
[7] S. Yim and K. Yi, "Design of an active roll control system for hybrid four-wheel-drive vehicles," *Inst. Mech. Eng., D, J. Automobile Eng.*, vol. 227, no. 2, pp. 151–163, 2013.
[8] B. L. Boada, M. J. L. Boada, L. Vargas-Melendez, and V. Diaz, "A robust observer based on H filtering with parameter uncertainties combined with neural networks for estimation of vehicle roll angle," *Mech. Syst. Signal Process.*, vol. 99, pp. 611–623, Jan. 2018.
[9] M. Jalali, E. Hashemi, A. Khajepour, S.-K. Chen, and B. Litkouhi, "Model predictive control of vehicle roll-over with experimental verification," *Control Eng. Pract.*, vol. 77, pp. 95–108, Aug. 2018.
[10] Bosch Motorsport. (2018). *Acceleration Sensor MM5.10-R*. [Online]. Available: http://www.bosch-motorsport.de/content/downloads/Products/16727677195.html
[11] H. Aerospace. (2018). *HG1120 MEMS Inertial Measurement Unit*. [Online]. Available: https://aerospace.honeywell.com/en/~/media/aerospace/files/brochures/n61-1524-000-004-hg1120-mems-inertial-measurement-unit-bro.pdf
[12] S. Yim, "Design of preview controllers for active roll stabilization," *J. Mech. Sci. Technol.*, vol. 32, no. 4, pp. 1805–1813, 2018.
[13] S. Yim, "Active roll preview control with V2V communication," *Int. J. Automot. Technol.*, vol. 20, no. 1, pp. 169–175, 2019.
[14] M. Rahman and G. Rideout, "Using the lead vehicle as preview sensor in convoy vehicle active suspension control," *Vehicle Syst. Dyn.*, vol. 50, no. 12, pp. 1923–1948, 2012.
[15] S. Yim, "Preview controller design for vehicle stability with V2V communication," *IEEE Trans. Intell. Transp. Syst.*, vol. 18, no. 6, pp. 1497–1506, Jun. 2017.
[16] K. Nam, S. Oh, H. Fujimoto, and Y. Hori, "Estimation of sideslip and roll angles of electric vehicles using lateral tire force sensors through RLS and Kalman filter approaches," *IEEE Trans. Ind. Electron.*, vol. 60, no. 3, pp. 988–1000, Mar. 2013.
[17] X. Shen *et al.*, "Multi-vehicle motion coordination using V2V communication," in *Proc. IEEE Intell. Vehicles Symp.*, Jul. 2015, pp. 1334–1341.
[18] A. Akbari and B. Lohmann, "Output feedback $H\infty/GH_2$ preview control of active vehicle suspensions: A comparison study of LQG preview," *Vehicle Syst. Dyn.*, vol. 48, no. 12, pp. 1475–1494, 2010.
[19] P. Li, J. Lam, and K. C. Cheung, "Multi-objective control for active vehicle suspension with wheelbase preview," *J. Sound Vib.*, vol. 333, pp. 5269–5282, Oct. 2014.
[20] Cohda Wireless, Cohda Wireless Pty. Ltd. (2015). *MK5 V2X on Board Unit*. [Online]. Available: www.cohdawireless.com
[21] S. Yim, C. W. Lim, and O. Myung-Hwan, "An investigation into the structures of linear quadratic controllers for vehicle rollover prevention," *Proc. Inst. Mech. Eng., D, J. Automobile Eng.*, vol. 227, no. 4, pp. 472–480, 2013.
[22] S. Yim, "Unified chassis control with electronic stability control and active front steering for under-steer prevention," *Int. J. Automot. Technol.*, vol. 16, no. 5, pp. 775–782, 2015.

Authors' photographs and biographies not available at the time of publication.